ckland, L. B., and L. R. Beuchat, eds. 1987. *Water Activity, Theory and Applications to Foods*. New York: Marcel Dekker.
ckland, L. B., and G. F. Stewart, eds. 1981. *Water Activity: Influences on Food Quality*. New York: Academic Press.
tchard, G. 1943. In *Proteins, Amino Acids, and Peptides*, R. Cohn and J. Edsall, eds. New York: Reinhold.
tchard, G., and J. G. Kirkwood, 1932. *Phys. Z.* **33**:297.
achman, H. K. 1959. *Ultracentrifugation in Biochemistry*, 226. New York: Academic Press.
ick, M. J. 1987. *Nonionic Surfactants Physical Chemistry*. 1003. New York and Basel: Marcel Dekker.
ulz, G. E., and R. H. Schirmer. 1979. *Principles of Protein Structure*. New York, Heidelberg, Berlin: Springer-Verlag.
er, J. C., and J. G. Kirkwood, 1931. The van der Waals forces in gases. *Phys. Rev.* 37:682-697.
er, A. K., and M. G. Phillips. 1986. A new determination of the structure of water t 25°C. *Chem. Phys.* **107**:47-60.
skal, E. O., and J. E. Tanner. 1965. Spin diffusion measurements: Spin echoes in he presence of a time-dependent field gradient. *J. Chem. Phys.* **42**:288-292.
n, O. 1924. Zur Theorie der Elektrolytischen Doppelschicht. *Z. Elektrochem.* 0:508-516.
es, R. H., and R. A. Robinson, 1948. Ionic hydration activity in electrolyte solutions. *J. Am. Chem. Soc.* **70**:1870-1878.
es, R. H., and R. A. Robinson. 1949. *Ann. N.Y. Acad. Sci.* **51**:593.
ord, C. 1957. The location of electrostatic charges in Kirkwood's model of organic ons. *J. Am. Chem. Soc.* **79**:5348-5352.
ord, C. 1961. *Physical Chemistry of Macromolecules*, 227, 293, 352, 563. New ork: Wiley.
sheff, S. N., and B. D. Coleman. 1960. On light-scattering studies of isoionic roteins. *Arch. Biochem. Biophys.* **87**:63-69.
sheff, S. N., and M. J. Kronman. 1959. The extrapolation of light scattering data zero concentration. *Arch. Biochem. Biophys.* **83**:60-75.
sheff, S. N., H. M. Dintzis, J. G. Kirkwood, and B. D. Coleman. 1957. Light attering investigations of charge fluctuations in isoionic serum albumin solutions. *Am. Chem. Soc.* **79**:782-791.
den Berg, C., and S. Bruin. 1981. Water activity and estimation in food systems. *Water Activity: Influences on Food Quality*, L. B. Rockland and G. F. Stewart, s. New York: Academic Press.
r, V. L., et al. 1981. Osmotic pressure studies of concentrated serum albumin lutions. *J. Colloid Interface Sci.* **79**(2):548-566.
bu, P., I. C. Baianu, and P. H. Orr. 1991. Unique hydration behavior of potato arch as determined by deuterium nuclear magnetic resonance. *J. Food Sci.* (2):458-461.
erman, J. R., and W. E. Brittin. 1957. Nuclear magnetic resonance studies in ultiple phase systems: Lifetime of a water molecule in an adsorbing phase on silica. *Phys. Chem.* **61**:1328-1333.

7

Physical Chemistry in the Food Processing Pilot Plant

Michael F. Kozempel and Peggy Tomasula

NOMENCLATURE

c	coefficient	RI	refractive index of solution
C	solute concentration in the potato	RI_0	refractive index of initial solution
C_1	initial solute concentration in the potato	S	solute concentration in blanch water
C_e	equilibrium solute concentration within the potato	S_1	solute concentration in entering blanch water
C_p	heat capacity	T	temperature
D	effective diffusion coefficient, reactor diameter	t	time
$dP/d\theta$	flow rate of mash	T_a	ambient or dry-bulb temperature
F	fraction of tracer fluid in exit stream	T_f	equilibrium mash temperature
h	convective heat transfer coefficient to air	T_s	steam temperature
I	internal age distribution	T_w	wet-bulb temperature
L	reactor length, drum width, nominal thickness of cut pieces	V	volume of the blanch water
m	molality, number of terms in equation (7-4)	W	water flow rate
M	moisture content of potato	x	diffusion path
P	potato flow rate	Δr	mash thickness
R	gas constant, radius of drum dryer	δH	differential heat of solution
		δx	small distance of travel on drum surface
		θ	reduced residence time
		λ	latent heat of vaporization
		ρ	density of the blanch water

τ residence time of the hot-water blancher

ω drum speed, rpm

The principles of physical chemistry apply to both pilot plant or commercial processing as well as to the laboratory. The problem is identifying the significant principles that control processes from the myriad of confounding, nonsignificant parameters. It is only with the advent of the computer that it is possible to handle a sufficient number of variables to properly account for some of the principles involved. The confounding parameters may be referred to as *nonidealities*. For example, deviations from laboratory results may appear because flow patterns in large pilot plant or commercial-scale reactors are rarely simple (perfectly mixed, or perfectly plug, flow). The actual flow pattern may cause difficult temperature control or lower reaction yields than expected for a simple flow. In addition, food processing systems are *rarely homogeneous*. These systems are usually of the following varieties: gas–liquid, as in evaporative concentration; gas–solid, as in convection drying; or, liquid–solid, as in a leaching process. Catalytic components (i.e., enzymes) are usually unstable under processing conditions. It is the determination of the controlling physical chemical principles to which much of pilot plant research is addressed. The application of physical chemistry in the pilot plant usually involves developing *mathematical models*. Using the appropriate physical chemical laws as a basis, the models aid the engineer in achieving a greater understanding of a process and permit extrapolation to processing conditions for which many of the controlling variables cannot be readily measured experimentally in the laboratory.

Consider the drying of a bed of potato slices in a commercial tunnel dryer. In this process, internal moisture from the drying potatoes diffuses to the surface, where it evaporates. Because of the variability in the raw material (potatoes), each slice is a different size, shape, and composition; there are air gaps between the slices; hence, air flow and contact is nonuniform. There is enzymatic and nonenzymatic browning. If the bed is fairly uniform, it is possible to determine an appropriate drying mechanism and to calculate the drying rate for an existing dryer from parameters dependent on measured process conditions. To design a new dryer, mathematical models for drying must include mass and energy balances for the dryer and the slices. The main variables are the temperature and moisture content of the potato slices leaving the dryer plus the drying time and temperature of the dryer.

Physical property data such as heat and mass transfer coefficients, heat capacities, thermal diffusivities, and shrinkage data are required in the drying of fruits and vegetables. Although some data are available in the literature (Singh, 1982; Balaban, 1988), it must usually be estimated because the variability between individual pieces due to cultural practices, cultivar, maturity, soil type, area where grown, environment, and storage conditions after harvest, makes it time-consuming and costly to compile data. Correlations based on generalized methods are often used (Rotstein, 1990). The real examples that follow give a better understanding of the application of physical chemistry in pilot plant research.

MIXING

An overriding phenomenon associated with almost all pilot plant processing is concerned with flow patterns during mixing and mass transport. Mass and energy transfer are dependent to a great extent on *mixing*. The principles governing mass and energy transfer are based on the assumption of perfect mixing, something that can only be achieved in a practical sense in the laboratory and approached in the pilot plant. Therefore, it is necessary to determine the actual mixing or flow pattern to develop a model for the real situation.

An excellent treatment of the theory of *residence time distribution* (RTD) is presented in Levenspiel (1972). It is assumed that actual flow patterns range between the ideal states of backmixing and plug flow, and may be modeled by a combination of backmixing and plug flow elements with dead regions and bypassing.

Backmixing is complete or perfect mixing, in which flow is turbulent and $L/D = 1$, where L is vessel length and D is vessel diameter. All fluid elements in the vessel have the same intrinsic properties, for example, concentration, temperature, and dwell time.

Plug flow is normally achieved in pipes under fairly high flow rates with Reynolds numbers greater than 10,000 and L/D ratios greater than 50. There is no axial mixing. It may be thought of as perfect radial mixing in a pipe or a series of infinitely small backmix reactors.

"Dead water" is thought of as fluid that moves slower relative to the fluid bulk or as a stagnant region in a vessel. It is caused by regions in the vessel that are virtually *unmixed*. Bypassing results when some of the fluid moves faster than the bulk of the fluid. Here the fluid does not mix (opposite of dead water), but simply passes through the vessel with no interaction with the bulk of the fluid. In the pilot plant none of these extremes would normally be encountered. All mixing would be a combination of two or more of these mixing patterns.

Generally, there are two problems associated with characterizing fluid mixing in a vessel. How is the RTD determined, and how are the results applied mathematically to the process under study? (In some cases, it may be necessary to treat the micromixing patterns, but normally characterizing macromixing is sufficient.) A simple way to experimentally measure RTD is with a *tracer* that is naturally part of or similar to the fluid component of interest.

For example, in developing a process for a cocoa butter substitute, it was

necessary to determine the RTD of the fractional crystallization system. Fat was used as the tracer. The RTD determination was started by establishing a steady-state flow of fat and solvent through the crystallizing system and maintaining temperature sufficiently high to avoid crystallization. At steady state there was no change in concentration, as monitored by the refractive index (*RI*). At zero time, the fat feed was replaced with a solvent (fat-free) feed, and the effluent refractive index (concentration of fat) was recorded for twice the nominal residence time. Dividing the *RI* by RI_0 gives *F*, the *fraction of tracer fluid* in the exit stream, with *I* equal to 1 − *F*:

$$F = \frac{RI}{RI_0} \tag{7-1}$$

$$I = 1 - F \tag{7-2}$$

The resulting data were plotted as *I*, the internal age distribution function, versus the *reduced residence time*, θ, as shown in Figure 7-1. The figure indicates the type of flow pattern, assuming the actual mixing can be represented as a mix of two ideal flow patterns. In the cocoa butter substitute study the flow pattern was best represented by the combination *backmixing* and *plug flow*. The

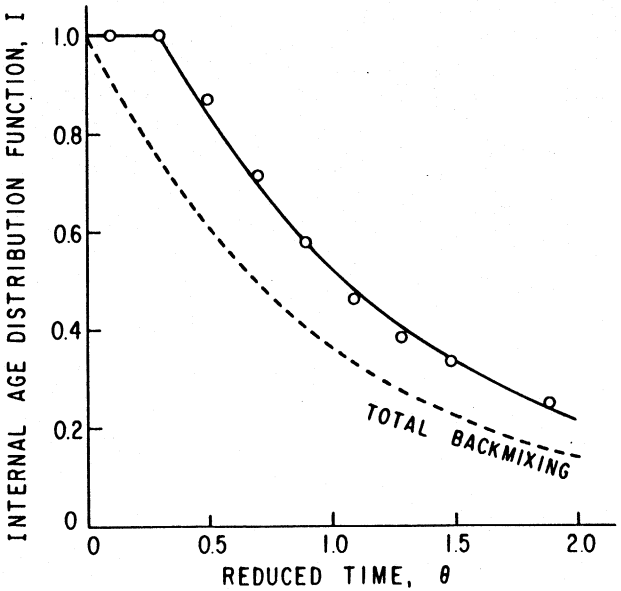

FIGURE 7-1. Residence time distribution study for fractionating tallow.

horizontal line at *I* = 1 is plug flow, and the exponential decay curve corresponds to backmixing. Using one of the simple flow models found in Levenspiel (1972) to describe the curve, indicated that there was 74% backmixing and 26% plug flow.

This was desirable for this particular process. The crystallization step was very quick, about 10 minutes. A large source of nuclei were needed to produce the proper crystals so quickly. Plug flow would contain no nuclei, and the process would be expected to give unsuitable crystals due to spontaneous nucleation. With this large amount of backmixing there were sufficient nuclei present. In scale-up, backmixing would be a critical parameter to keep constant.

In a study of hot-water blanching of potatoes, a tracer was added to the feed stream, as opposed to the previous example in which the drop in tracer concentration was followed after tracer addition was terminated. To study the flow patterns in a hot-water blancher for blanching, a steady-state blancher operation was established with plain water, that is, the blancher was operated as if potatoes were being blanched, even though no potatoes were fed into it. At time equal zero, a lactose solution was fed in, and its concentration was followed at the exit of the blancher. Again, *RI* was a convenient way to follow the tracer. The flow pattern closely matched the same model—a mixed model of backmixing and plug flow.

Another method of applying the results of the RTD mathematically to the process under study is by treating the fluid stream as the sum of ideal streams, for example, backmixed, plug flow, dead water, or by-pass. The ideal streams are treated separately and then combined. An example of this method is described in the next section.

DIFFUSION

In potato processing, potato pieces go through a hot-water bath or blancher to leach sugars (especially reducing sugars, such as glucose) that contributes to nonenzymatic browning (Talburt and Smith, 1987). Sugars diffuse from the interior of the potato pieces to the surface, where they dissolve in the hot water. However, the rate-controlling step could be mass transfer at the surface, due to resistance at the boundary layer, or *diffusion* through the piece. What controls the rate of leaching, and how is the rate-controlling step and its mechanism determined?

A diagram of the pilot plant equipment is shown in Figure 7-2. Water was circulated through a heat exchanger to the blancher and back, as shown. The potatoes were passed through the blancher in small baskets, the basket rate of travel through the blancher simulating potato flow rate. The concentration of glucose and potassium in the exit water was monitored.

Because of the high recycle rate this system closely resembled an ideal *con-*

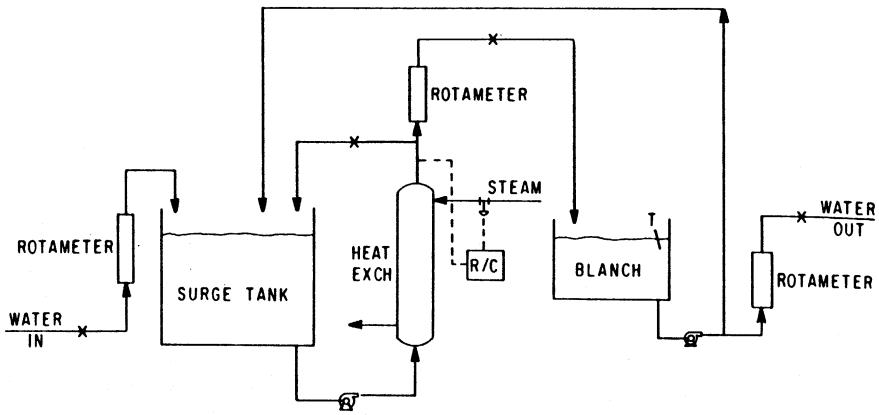

FIGURE 7-2. Process for simulating blanching potatoes.

tinuous-flow stirred-tank reactor (CSTR), or backmix reactor, with complete backmixing and uniform temperature. Although glucose was the component of interest, potassium concentration was used as a flow tracer. Glucose in the water samples is subject to bacterial degradation, but potassium can be readily analyzed even if all potato solids were to decompose. Typical experimental data are shown in Figure 7-3.

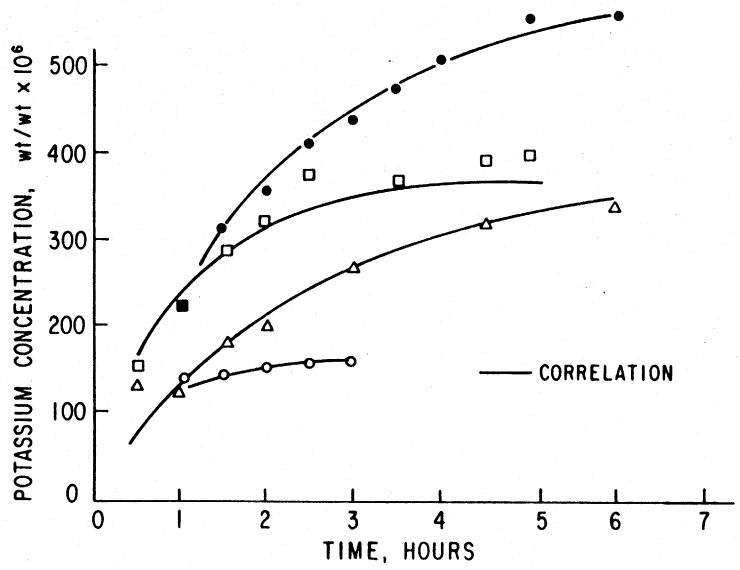

FIGURE 7-3. Correlation of potassium concentration in blancher water vs. processing time.

The experimental data were best represented by a *diffusion model*. Mass transfer at the surface was found to be insignificant. Diffusion in potatoes may be represented by *Fick's second law:*

$$\frac{\delta C}{\delta t} = D\frac{\delta^2 C}{\delta x^2} \tag{7-3}$$

A. B. Newman (1931) presented a simple series expansion to solve the partial differential equation of Fick's law for a French fry strip of potato:

$$C = C_e + (C_1 - C_e)\frac{8}{\pi^2}\sum_{m=0}^{\infty}\frac{1}{(2m+1)^2}\exp\left[-D(2m+1)^2\pi^2\frac{\tau}{L^2}\right] \tag{7-4}$$

Use of this model assumes that the potato consists of an *insoluble* and *isotropic matrix of starch*, the *major solid component of the potato*, and other solid components (such as pectin), and a liquid component—water. Equating C_e to the solute concentration in the water, S, and making a mass rate balance over the hot-water blancher (Kozempel et al., 1981a), the predicted or theoretical values of potassium concentration in the blanch water (also other diffusing components such as glucose) can be calculated from

$$PMC_1\left[1 - \frac{8}{\pi^2}\exp\left(-\frac{\pi^2 D\tau}{L^2}\right)\right] - PMS\left[1 - \frac{8}{\pi^2}\exp\left(-\frac{\pi^2 D\tau}{L^2}\right)\right] + W(S_1 - S) = \left[V\rho + \frac{PM\tau}{2}\left(1 - \frac{8}{\pi^2}\exp\left(-\frac{\pi^2 D\tau}{L^2}\right)\right)\right]\frac{dS}{d\theta} \tag{7-5}$$

Assuming uniform temperature, piece size, and complete backmixing the value of the *effective diffusion coefficient, D*, may be calculated from equation (7-5). The D is termed an effective diffusion coefficient because the potato is not truly isotropic; its value is influenced by other diffusing components of the potato and the diffusional path. To determine the value of D from the data of Figure 7-3, a pattern optimization program was used. The correlation coefficients for the curves in Figure 7-3 were 0.9 or above.

Having established diffusion as the controlling step for leaching during blanching, the research went in two directions. At the bench level, Tomasula and Kozempel (1989) determined the variation of the diffusion coefficients of glucose, potassium, and magnesium in potatoes with temperature. At the bench, the effect of flow on leaching can be controlled to get "true" effective diffusivities. The data showed a change in slope at the gelatinization temperature (60°–

65°C). Effective diffusion coefficients were correlated with reciprocal temperature over three temperature ranges using an Arrhenius-type equation over the full temperature range (45°–90°C) and a separate polynomial with temperature-dependent coefficients for the ranges (45°–60°C and 65°–90°C).

Effective diffusion coefficients for various solids encountered in food processing also are given by Schwartzberg and Chao (1982).

Concurrently, potato-slice-blanching research was scaled up to the large pilot scale. In the pilot plant (Fig. 7-2) work discussed previously, the water flow pattern through the blancher nearly approximated complete backmixing (CSTR), and was correlated by a model representing the flow as 94% backmixed and 6% plug flow. At the larger scale (875 liter) less thorough mixing in the blancher was expected, more nearly duplicating commercial scale blanchers.

To determine the flow pattern in the larger pilot plant unit operating at steady state, a lactose tracer solution was fed at time equal zero, and the exit concentration was monitored by refractive index as a function of time. Using the models given in Levenspiel (1972), the flow was found to consist of 78% backmixed and 24% plug flow, as shown in Figure 7-4 (Kozempel et al., 1985).

To calculate leaching using the plug flow model, the blancher was arbitrarily separated into *mixing zones* with the width of the zones equal to the pitch of the screw used to move the potatoes through the blancher. The temperature of a single site in each zone was monitored and was found to be *uniform* within the zones. The blanch model was applied sequentially to each zone at the temperature of the zone using the exit concentration of the previous zone as the inlet concentration. This plug flow model was applied to 24% of the flow stream in the blancher.

Temperature and concentration are uniform in backmixing. Therefore, the blancher exit temperature was used for the backmix contribution, and the backmix model was applied to 76% of the flow in the blancher (Kozempel et al., 1985).

Another identified complication is piece size. In the pilot plant tests piece size was fairly uniform. Figure 7-5 illustrates a typical piece-size distribution encountered in the pilot plant process. Since distribution is somewhat random and the increased difficulty of making iterative calculations for each piece size does not warrant the increased effort, an average piece size was used.

SOLUBILITY

Separation by fractional crystallization depends upon the relative solubility of the solutes. In simple cases, each solute is considered independent of the other solutes. A solubility curve must be established to design a fractional crystallization process. Over small temperature intervals, for solutions in which there

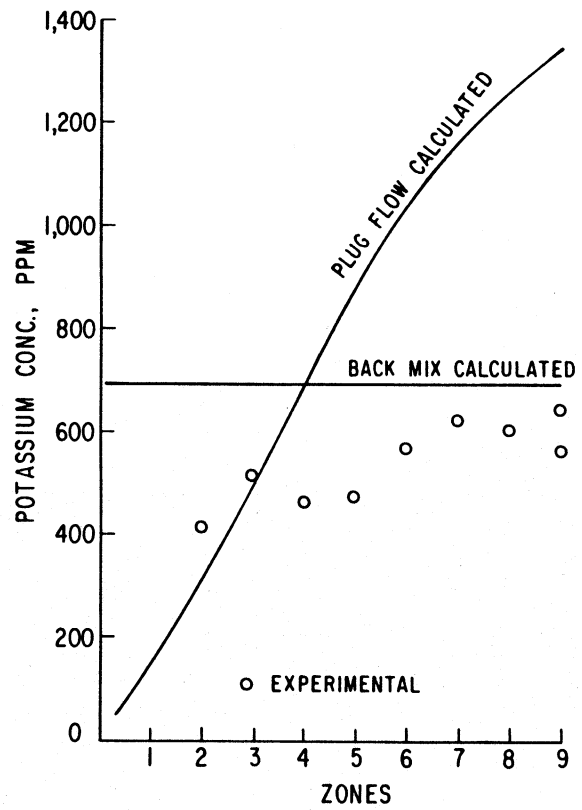

FIGURE 7-4. Comparison of experimental potassium concentration with concentration calculated assuming back mix or plug flow in pilot plant.

is no change in the nature of the solute, the solubility can be correlated using equation (7-6) (Kozempel, 1971).

$$\ln m = -(\delta H/R)(1/T) + c \qquad (7\text{-}6)$$

In some food systems, for example, in fat-containing systems, the interaction of the various solutes or individual fractions may be very important. An example of this is seen in the process (Fig. 7-6) to fractionally crystallize beef tallow into a cocoa butter substitute. The solubility of beef tallow in acetone, curve *A* in Figure 7-7 (Kozempel et al., 1981b), was determined to develop a process for fractionating tallow to obtain a cocoa butter substitute. However, in attempting to establish the temperature for fractionating (crystallizing) the

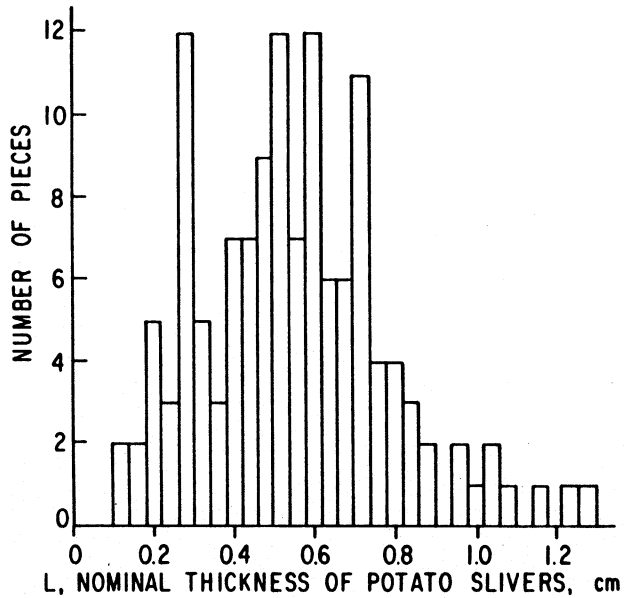

FIGURE 7-5. Distribution of piece sizes in a commercial hot-water blancher.

stearine or high melting fat fraction, the process did not follow the solubility curve as expected.

For example, starting with a tallow concentration of 0.093, crystallization began at 29°C. The concentration of the filtrate did not follow solubility curve *A*, but followed line *B*1 instead (Fig. 7-7).

Starting with a different initial concentration, the filtrate concentration (crystallization) followed a different line, for example, *B*2. Although it is well known that solubility depends on the temperature of a system and not the initial concentration, these data gave every indication that, in this system, solubility depends on the initial concentration.

The explanation of this apparently anomalous solubility behavior stems from the nature of beef tallow. It is composed of many different triglycerides. Curve *A* establishes the solubility of the highest melting or least soluble component of the original mixture. As crystallization proceeds, the filtrate solution is stripped of the highest melting crystallizing fat, and curve *A* no longer applies to the liquid. Instead, crystallization is governed by a different solubility curve corresponding to a new least soluble fraction (curve *A'*, Fig. 7-7). As this component crystallization continues, solubility becomes governed by the next least soluble component. In essence, an operating line is established by the intersections of the temperature with the family of solubility curves. It is reasonable to

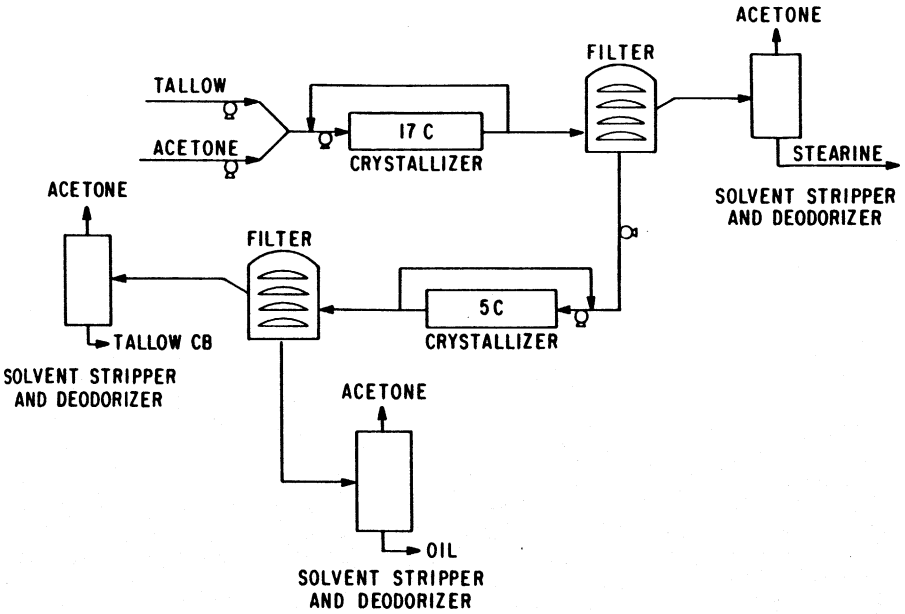

FIGURE 7-6. Process flow sheet for fractionating tallow.

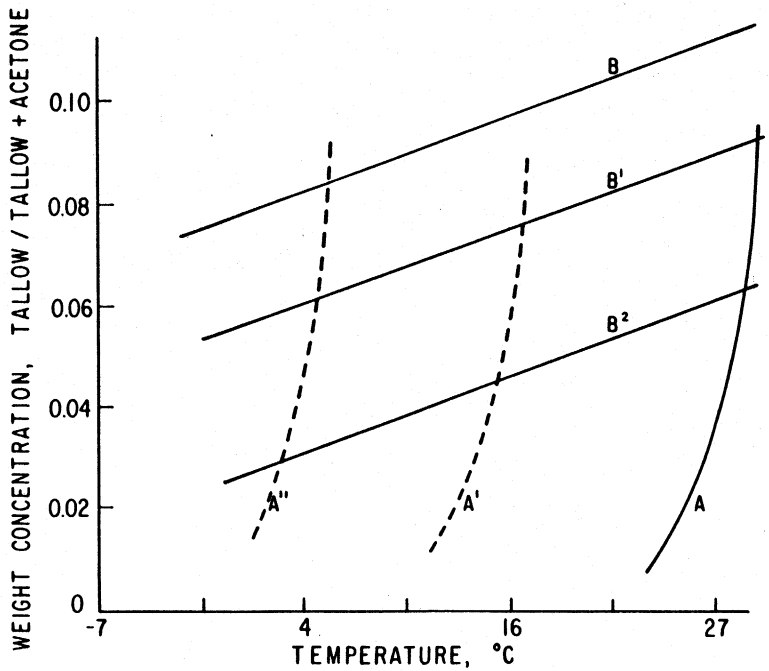

FIGURE 7-7. Solubility diagram for tallow in acetone.

expect that the various solubility curves and various operating lines would be parallel, since there is just a slight difference in the components.

The changing composition problem can be overcome by a systematic experimental procedure. First, an initial solubility curve must be determined. Next, one of the operating lines must be established by successively crystallizing a fat solution. From these curves, other operating lines are established parallel to the first, and the process is designed using the family of operating lines and the initial solubility curve.

In the cocoa butter substitute study, the solution was crystallized in acetone until the temperature reached 16–18°C, which separated the stearin fraction, a fraction useful as shortening or hard butter. This crystallization process nominally corresponded to a path defined by the intersection of the operating line with solubility curve A'.

Further cooling to a nominal 5°C produced a crystallized fraction with composition and physical properties almost identical to cocoa butter. This crystallization nominally corresponded to the intersection of the operating line with solubility curve A''. The filtrate was a liquid at room temperature, useful as a deep-fat frying oil.

DRUM DRYING

The mathematical treatment of *drum drying* was considered impractical before the advent of the computer. Attempts to formulate and solve the mathematical equations failed because of the great number and interrelationships of the variables.

Instant mashed potatoes or potato flakes are dried on a single drum dryer. The pretreatment of the potatoes has a strong influence on the performance of the dryer and the quality of the product. Therefore, it was necessary to model the preprocessing steps as well. Not only is every piece of potato slightly different (size, moisture content, starch composition, texture), but there are significant variations in cooked potato properties (per piece and within the mash). Also, the drum surface is not perfectly uniform. There are irregularities, hot spots, and end effects (at the sides of the drum where the side of the heated surface is exposed to the air and not coated with drying mashed potato).

Figure 7-8 is a sketch of the side view of a single drum dryer. Mash is loaded onto the drum surface at zero degrees of rotation and the dried flakes are doctored off at about 295 degrees of rotation. The pilot plant unit has four spreader rolls. The basic equation describing the drying can be developed from an energy balance over an infinitesimal volume, Figure 7-9, of mash of cross section L and r by δx (Kozempel et al., 1986).

The flow rate of mash is $dP/d\theta$ (kilogram mash/hour). Thus, $d^2P/d\theta^2$ is the change in mash flow rate, or the drying rate. The drying rate is expressed

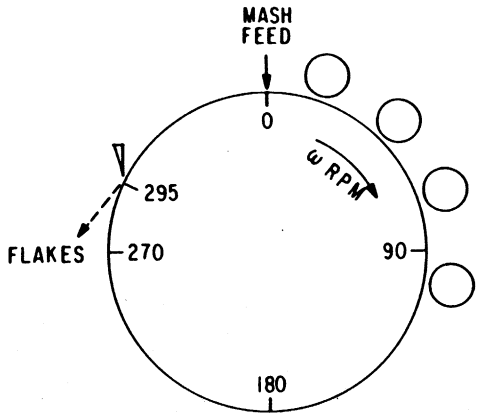

FIGURE 7-8. Side view of drum dryer.

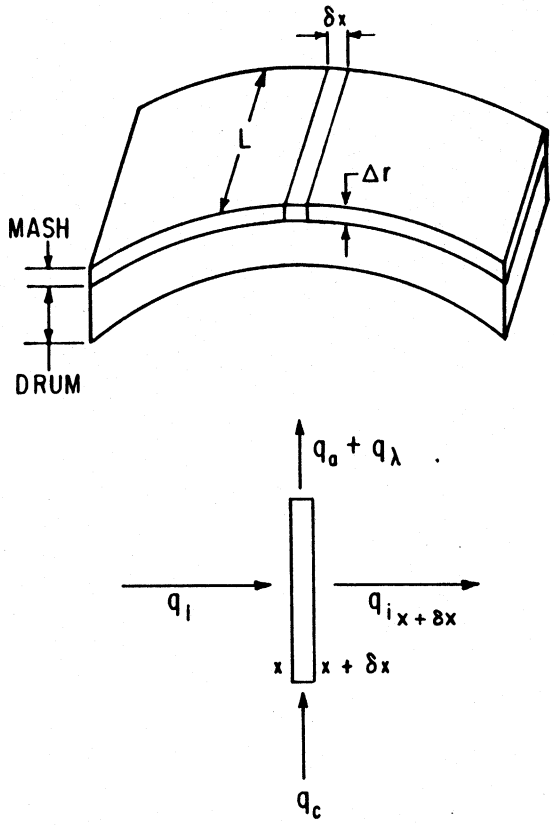

FIGURE 7-9. Diagram of drum and mash sheet for modeling drum dryer.

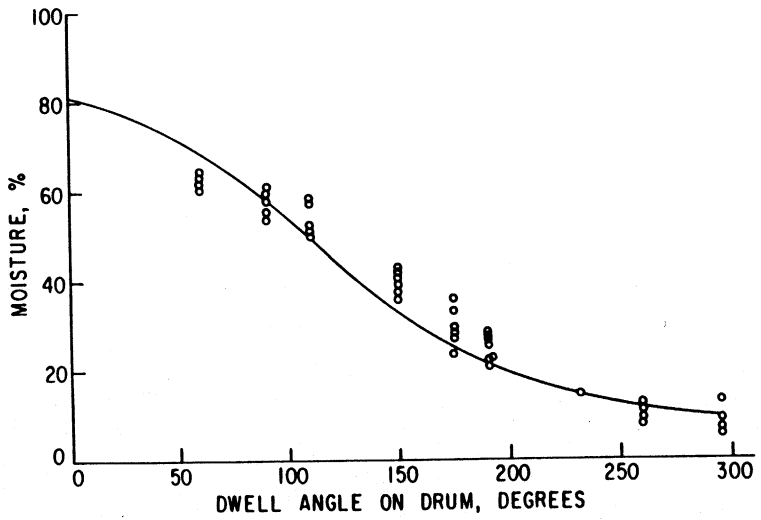

FIGURE 7-10. Typical plot of drum dryer experimental data and correlation curve for moisture vs. position on drum surface.

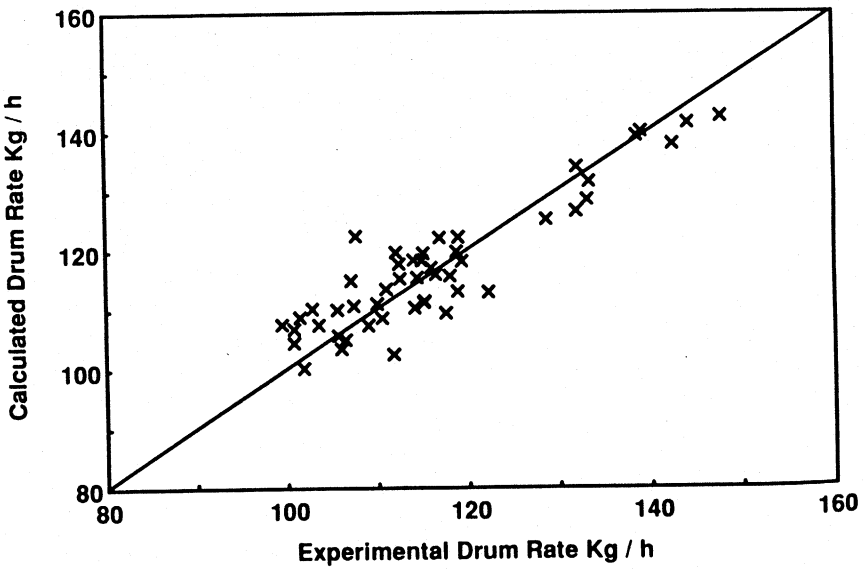

FIGURE 7-11. Plot of calculated vs. experimental drum dryer rate for two processing seasons.

as

$$\frac{-d^2P}{d\theta^2} = \frac{hML(T_s - T) - hM\left(\frac{T_sT_f}{T_f - T_a}\right)L(T - T_a)}{\frac{\lambda + CpT}{2\pi R\omega}} \tag{7-7}$$

Solving this equation requires the solutions of several auxiliary equations. The temperature of the mash can be calculated from the wet-bulb temperature, the equilibrium mash temperature, and the moisture as in equation (7-8).

$$T = T_w + (T_f - T_w)\exp(-cM) \tag{7-8}$$

The equilibrium mash temperature depends on the wet-bulb temperature and steam pressure

$$T_f = T_w + 99.11 + 5.12 \times 10^{-5}\ (\text{steam pressure}) \tag{7-9}$$

In addition, to evaluate equation (7-7), the initial condition for the flow rate $(dP/d\theta)_0$, which is the capacity of the drum dryer, is needed. The mash flow rate depends on drum speed (rpm), steam pressure, number of spreader rolls, degree of cooking, starch content, bulk density of the dry potato, and the texture of the raw potato (Kozempel et al., 1990).

By using a *Hook–Jeeves pattern search* for the best values of the coefficients, a model that successfully predicts the moisture and capacity (drum dryer feed rate or $(dP/d\theta)_0$) was developed for drum drying potato flakes, as shown in Figures 7-10 and 7-11.

References

Balaban, M. 1988. Comparison of models for simultaneous heat and moisture transfer in food with and without volume change. Paper presented at the AIChE National Meeting, Denver, Colo., August 21–24.

Kozempel, M. F. 1971. Viscosity, solubility, density of isopropenyl stearate and isopropenyl acetate. *J. Chem. Eng. Data* **16**(3): 345–346.

Kozempel, M. F., J. F. Sullivan, and J. C. Craig, Jr. 1981a. Model for blanching potatoes and other vegetables. *Lebensmittel-Wissenshaft u.-Technol.* **14**:331–335.

Kozempel, M. F., J. C. Craig, Jr., W. K. Heiland, S. Elias, and N. C. Aceto. 1981b. Development of a continuous process to obtain a confectionery fat from tallow: Final status. *J. Am. Oil Chem. Soc.* **58**(10):921–925.

Kozempel, M. F., J. P. Sullivan, and J. C. Craig, Jr. 1985. Modeling and simulating commercial hot water blanching of potatoes. *Amer. Potato J.* **62**:69–82.

Kozempel, M. F., J. F. Sullivan, J. C. Craig, Jr., and W. K. Heiland. 1986. Drum drying potato flakes—A predictive model. *Lebensmittel-Wissenshaft u.-Technol.* **19**:193-197.

Kozempel, M. F., P. M. Tomasula, J. C. Craig, Jr., and M. J. Kurantz. 1990. Effect of potato composition on drum dryer capacity. *Lebensmittel-Wissenshaft u-Technol.* **123**:312-316.

Levenspiel, O. 1972. *Chemical Reaction Engineering*, 2d ed. New York: Wiley.

Newman, A. B. 1931. The drying of porous solids: Diffusion calculations. *Trans. Amer. Inst. Chem. Eng.* **27**:310-333.

Rotstein, E. 1990. Drying of foods. In *Biotechnology and Food Process Engineering*, H. G. Schwartzberg and M. A. Rao, eds. New York: Marcel Dekker.

Schwartzberg, H. G., and R. Y. Chao. 1982. Solute diffusivities in leaching processes. *Food Technol.*: 73-86.

Singh, R. P. 1982. Thermal diffusivity in food processing. *Food Technol.*: 87-91.

Talburt, W. F., and O. Smith. 1987. In *Potato Processing*, 4th ed. New York: Van Nostrand Reinhold.

Tomasula, P., and M. F. Kozempel. 1989. Diffusion coefficients of glucose, potassium, and magnesium in Maine Russet Burbank and Maine Katahdin potatoes from 45 to 90°C. *J. Food Sci.* **54**:985-989, 1046.

8

Rheology of Cheese

Michael H. Tunick and Edward J. Nolan

WHY RHEOLOGY IS USED IN CHEESE ANALYSIS

The instrumental measurement of the rheological properties of cheese is performed for two reasons: as a *quality control* method for cheesemakers, and as a technique for scientists to study *cheese structure*. The rheological properties of cheese can be as important as flavor, and are a large part of the total score awarded by the cheese grader (Farkye and Fox, 1990). Consequently, an objective instrumental method of determining rheological properties of cheese would be quite valuable. This also holds true for scientific studies of cheese. The pH at whey draining affects the size and shape of protein aggregates and has a large effect on the textural properties of cheese (Fox, Lucey, and Cogan, 1990). Low-pH curds result in a crumbly texture, such as in Cheshire cheese, whereas high-pH curds lead to more elastic cheeses, such as Swiss or Gouda. The extent of proteolysis and the amounts of water, protein, fat, and salt in cheese also affect texture, resulting in profound differences between cheese types. Research into the origins of cheese texture is an important part of dairy science, and investigations into cheese rheology have been conducted for over half a century. Correlating the results of various instrumental tests to each other and to subjective evaluations by sensory panels and consumers is a goal that is constantly being strived for (Szczesniak, 1987).

BRIEF HISTORY OF RHEOLOGICAL MEASUREMENTS OF CHEESE

The three general categories of food texture measurement are empirical, imitative, and fundamental tests (Scott Blair, 1958). The idea behind empirical